CORA Cork Open Research Archive
Cartlann Taighde Oscailte Chorcaí

Title	Rheology and the Fe3+-chlorine reaction in basaltic melts
Authors	Webb, Sharon L.;Murton, Bramley J.;Wheeler, Andrew J.
Publication date	2014-02-01
Original Citation	WEBB, S. L., MURTON, B. J. & WHEELER, A. J. 2014. Rheology and the Fe3 +–chlorine reaction in basaltic melts. Chemical Geology, 366, 24-31. doi:10.1016/j.chemgeo.2013.12.006
Type of publication	Article (peer-reviewed)
Link to publisher's version	10.1016/j.chemgeo.2013.12.006
Rights	Copyright © 2014 Elsevier B.V. All rights reserved. - https://creativecommons.org/licenses/by-nc-nd/4.0/
Download date	2026-11-07 18:24:42
Item downloaded from	https://hdl.handle.net/10468/2469



UCC
University College Cork, Ireland
Coláiste na hOllscoile Corcaigh

Rheology and the Fe^{3+}-Chlorine Reaction in Basaltic Melts

Sharon L Webb[1], Bramley J Murton[2] and Andrew J Wheeler[3]

1 - Mineralogy Department, Goldschmidtstr., Georg-August University, 37077 Goettingen, Germany. swebb@gwdg.de

2 - Marine Geosciences Group, National Oceanography Centre, European Way, Southampton, SO14 3ZH, UK. bramley.murton@noc.ac.uk

3 - School of Biological, Earth & Environmental Sciences, University College Cork, North Mall, Cork, Ireland. a.wheeler@ucc.ie

Abstract

The viscosity of mid-ocean ridge basalt (MORB) as a function of halogen content was determined in the high viscosity range (10^9-10^{12} Pa s) using the micropenetration technique. In this study we show that, in the presence of iron, the addition of chlorine reduces the viscosity of a metaluminous melt (basalt); and that the addition of chlorine increases the viscosity of the analog iron-free haplo-basalt. Previous studies of the effects of chlorine and fluorine on the viscosity of peralkaline and metaluminous melts has shown that while fluorine decreases the viscosity of such melts, chlorine acts to increase their viscosity. The major effect of the addition of chlorine to the present basalt melt is the conversion of a network-forming Fe^{3+} to a network-modifying Fe^{2+} for each added Cl^- ion, resulting in an increase in Fe^{2+}/Fe^{tot} from 0.126 to 0.432 upon the addition of 1.41 mol% Cl_2O_{-1}, in air at a constant $\log_{10} fO_2$ of -0.7. It would appear that it is this increase in Fe^{2+} induced by the addition of chlorine, rather than the structural position of the chlorine atom in the melt which causes the reduction in viscosity. Of greater importance is that such an increase in Fe^{2+} would, in general, be interpreted as a 3 order of magnitude decrease in fO_2, instead of the addition of chlorine.

Keywords: chlorine, viscosity, redox, iron

Highlights

- The addition of chlorine to iron-free melts acts to increase melt viscosity
- The addition of chlorine to a melt reduces Fe^{3+} to Fe^{2+}
- The addition of chlorine to an iron-bearing melt results in a decrease in viscosity

1. Introduction

Basaltic magmas at the mid-oceanic ridge erupt under water and are quenched to glass or glass-bearing rock. This process results in the formation of pillow lavas, lava tubes, volcanic cones, low domes and flat topped volcanoes (see Briais *et al*., 2000; Stretch *et al*., 2006; Searle *et al*., 2010). The shape of the volcanic edifice formed is a function of the magma composition, temperature, crystal- and volatile-content – that is – the magma viscosity. The melt composition investigated here is that of a basaltic glass from a flat-topped volcano located at the mid-Atlantic ridge at 3 km below sea level.

There are increasing amounts of literature data on the viscosity of basaltic or near basaltic composition liquids, both with and without iron (e.g. Vetere *et al*., 2006; Vetere *et al*., 2007; Getson & Whittington, 2007; Vetere *et al*., 2008; Behrens & Hahn, 2009; Davi *et al*., 2009; Misiti *et al*., 2009; Misiti *et al*., 2011); with crystals (e.g. Villeneuve *et al*., 2008; Ishibashi & Sato, 2010; Hobiger *et al*., 2011) and varying water content (e.g. Whittington *et al*., 2000; Giordano & Dingwell, 2003; Whittington *et al*., 2009). There are no data on the effect of halogens on the viscosity of basaltic composition melts.

The effect of chlorine and fluorine on the rheology of basaltic composition melts is of importance as studies of the rheology of synthetic iron-free aluminosilicate melts have shown that chlorine increases melt viscosity (Baasner et al., 2013) in the high viscosity (10^8-10^{12} Pa s) range while fluorine has been found to always decrease the viscosity of all silicate melt compositions investigated in the literature (at both low and high viscosity conditions – e.g. Dingwell & Hess, 1998 - 67 mol% SiO_2 ; Baasner et al., 2013 – 67 mol% SiO_2). The study of Dingwell & Hess (1998) found that the addition of chlorine to an iron-bearing (aluminium-free) sodium-silicate melt resulted in a decrease in viscosity at the high viscosity range (but an increase in viscosity at low viscosities (10^2-10^5 Pa s)). The study of Zimova & Webb (2006 – 67 mol% SiO_2 with the halogens added as FeF_3 and $FeCl_3$) found in the viscosity range $10^{8.5}$ to 10^{12} Pa s, that chlorine increases the viscosity of peralkaline iron-bearing melts but decreases the viscosity of peraluminous iron-bearing melts in the high viscosity region. Therefore, the question of the effect of chlorine on the viscosity of geologically relevant melt compositions needs to be addressed.

Both chlorine and fluorine are found in MORB melts, with up to 0.07 wt% Cl in erupted basaltic glass and up to 0.31 wt% (~0.25 mol% Cl_2O_{-1}) in basaltic andesite glasses erupted at mid-oceanic ridges (Wanless *et al*., 2011). Similar amounts of F (0.02 wt %, ~0.03 mol% F_2O_{-1}) are found in mid-Atlanitic ridge glasses (Byers et al., 1986) and (0.06 wt% F) in the

"MORB-like" basalts from the Galapagos Archipelago plume (Koleszar *et al*., 2009). Other basaltic glasses have higher concentrations of halogens; e.g. 0.94 wt.% Cl, and 1.95 wt.% F in the Siberian Traps flood basalts (Black et al., 2012). In order to avoid the difficult interpretation of variations in viscosity based on the additions of small amounts of halogens, and the accompanying variations in melt composition, up to 1.4 mol% Cl_2O_{-1}, and 2.9 mol% F_2O_{-1} have been added to the present basalt composition melts.

2. Experiments

The basaltic composition is that of a MORB from the mid-Atlantic ridge. Crystal-free basaltic glass samples were obtained by an ROV (remotely operated vehicle) from the flat topped volcano located at 2993 m water depth (Station V24: 45° 28.7'N/27° 51.0'W) during the VENTuRE expedition aboard the national research vessel RV Celtic Explorer (Wheeler *et al*., 2011a; 2011b; 2013). The composition of the glass has been determined by electron microprobe, and is listed in Table 1. The composition is similar to that determined for basaltic glasses from the AMAR Valley (American Mid-Atlantic Ridge) (le Roex *et al*., 1996). A synthetic glass with the composition listed in Table 1 has been made from powdered oxides which had been dried at 200°C for 24 hours and then decarbonated at 800°C for 24 hours before being melted in air at 1250°C in a $Pt_{90}Rh_{10}$ crucible in a $MoSi_2$ furnace. The chlorine and fluorine were added as NH_4Cl and NH_4F in air to the synthesised glasses at 1250°C. There was ~60% loss of chlorine and ~2% loss of fluorine in this synthesis procedure. Glasses with up to 1 wt% of each halogen were produced. The resulting glass was removed from the crucible, crushed and remelted 3 times in order to homogenize the samples. Three mm thick, 8 mm diameter glass samples were cored out of the crucible. The ends of these cylinders were polished flat and parallel. More halogens than are found in natural samples were added to the melts in order to unambiguously determine their effect on melt viscosity.

The chemical composition of the synthetic glasses used in the experiments was determined by a combination of electron microprobe and wet-chemistry. The electron microprobe data are shown as atom% in Table 2. The wet-chemistry analysis was done in two steps. The Fe^{2+} content of the glasses was determined by manganometric titration of the glasses dissolved in a mixture of HF and H_2SO_4. Samples of the glasses were also dissolved in a solution of HF, HCl, ortho-phenanthrolin, ascorbic acid and Na-acetate. This procedure resulted in the oxidation of all of the iron in solution to Fe^{3+}. The resulting Fe^{3+} content was measured by spectral photometer. Using this information, the Fe^{2+}/Fe^{tot} of the glass could be calculated. As the wt% Fe_2O_3 determined by wet chemistry was slightly different to that determined by

electron microprobe (see Table 3), the Fe^{2+}/Fe^{tot} value was taken from the wet chemistry data and applied to the microprobe Fe analysis to give the absolute values of FeO and Fe_2O_3 in the glasses (see Table 3). The water content in ppm by weight of the nominally dry samples was determined using mid infrared (MIR) spectroscopy using the Paterson method (Paterson, 1982). These data are shown in Table 3. The water content (65-255 ppm) of these glasses is comparable to that of the peraluminous halogen-bearing glasses (29-113 ppm) of Baasner et al. (2013) which were synthesized by the addition of NaCl, NaF, CaF_2 and $CaCl_2$ rather than the ammonium compounds used in the present study; and also, for example, comparable to the 200 ppm water content of the nominally anhydrous halogen-free peralkaline rhyolite glasses of Di Genova et al. (2013).

The densities of the glasses were measured at room temperature using the Archimedean method in ethanol. The densities are given in Table 3.

The heat capacity of the glasses and melts were determined in a Netzsch 404 C DSC for a cooling- and heating-rate of 20 K min^{-1}. The calorimeter was calibrated using the data from a 113.135 g single crystal Al_2O_3 and the data of Robie et al. (1978). The heat capacity curves are shown in Fig. 1.

The viscosity of the melts was determined by micropenetration in a Netzsch 402 dilatometer over the range $10^{8.5}$ - 10^{13} Pa s. The principle of this type of rheology measurement is to force a single crystal sapphire sphere with known diameter into the melt at a fixed temperature and applied force. Two mm diameter Al_2O_3 spheres were used with the applied force ranging from 0.1 to 10 N. The larger forces are used at the higher viscosity range. Viscosity is determined by measuring the indent distance of the sphere as a function of time by:

$$\eta = \frac{0.1875\ F\ t}{\left(r\ l^3\right)^{0.5}} \quad (1)$$

for F – applied force, t – time, r – radius of the sapphire sphere, l – indent distance and 0.1875 – a geometric constant determined by Pocklington (1940) for a spherical indenter. The accuracy and precision of the viscosity measured using this method was determined from measurements of the viscosity of the standard glass DGG-1 (Na_2O-CaO-SiO_2 glass from the Deutsche Glastechnische Gesellschaft). The measured viscosity values across the temperature range 520 – 620°C and viscosity range $10^{8.5}$- $10^{12.0}$ Pa s were found to be within less than ±0.06 $\log_{10}$ units of the standard tables. The temperature at the sample position ±5 mm within the dilatometer was calibrated via the melting temperatures of Bi (271.4°C), Zn

(419.6°C), Al (660.3°C), NaCl (801°C) and Ag (961.5°C). The error in the temperature measured by the Type S thermocouple using this calibration method is ±0.5°C. The viscosity data are given in Table 4 and shown in Fig. 2.

The parameters of the Arrhenian equation:

$$\log_{10} \eta = A + \frac{B}{T} \quad (2)$$

for T – temperature in K, which describe the data are given in Table 5.

3. Results and Discussion

3.1 Density

The effect of chlorine and fluorine on density of the glasses is shown in Fig. 3. Although there is a small effect on density due to the different limiting fictive temperatures (T_f) for the different composition melts, and there are very few data, it is of interest to calculate the partial molar volumes of F_2O_{-1} and Cl_2O_{-1} in these glasses. The partial molar volumes of the components Cl_2O_{-1} and F_2O_{-1} were calculated from a multiple linear regression

$$V(X) = \sum V(X_i) \quad (3)$$

for X_i – mole fraction of the component and V_i – partial molar volume of the component, and are shown in Table 6. As discussed below, the addition of chlorine (and fluorine) results in an increase in Fe^{2+}/Fe^{tot} of the glass. Therefore, it was necessary to include the components FeO and Fe_2O_3 in the partial molar volume calculation. The extra density data point needed for a multiple linear regression of the volume data comes from a piece of the starting glass which was remelted at FMQ conditions. This glass has an Fe^{2+}/Fe^{tot} = 0.565 and a density of 2.796±0.003 g cm^{-3}. There are no available data for the partial molar volumes of FeO and Fe_2O_3 in glasses, however, the present values compare well with the data of Liu and Lange (2006) for the partial molar volume of FeO (13.92 cm^3 mol^{-1}) and Fe_2O_3 (41.52 cm^3 mol^{-1}) in silicate liquids at 1400°C. The partial molar volume of F_2O_{-1} calculated for the present glass (3.22 cm^3 mol^{-1}) is much smaller than that calculated by Dingwell et al. (1993) in a haplogranitic melt at 750°C to be 14.2 cm^3 mol^{-1}. However, as seen in the Fe^{2+}/Fe^{tot} data (Table 3, Fig. 4) chlorine in the presence of fluorine appears to have a different effect on

Fe^{2+}/Fe^{tot} than chlorine alone. This suggests that the structural position of chlorine (and therefore its partial molar volume) depends on the presence or absence of fluorine.

3.2 Calorimetry

The limiting fictive temperature (T_f) for each glass was calculated from the heat capacity data using the method of Moynihan et al. (1976). This calculation requires the determination of the theoretical glass heat capacity at temperatures above the glass transition. The Maier-Kelley equation:

$$C_{pg}=a+bT+cT^{-2} \qquad (4)$$

with temperature in K, (Maier & Kelley, 1932) was fit to the glass part of the heat capacity curve from 200°C to the onset of the glass transition peak and was used to extrapolate the data to higher temperatures. The calculated T_f values for each glass are given in Table 3.

The changes in configurational heat capacity (C_p^{conf}) as a function of chlorine content were also calculated by extrapolating the Maier-Kelley equation to temperatures above the glass transition. The configurational heat capacity was then calculated as the difference between the heat capacity of the melt and the extrapolated heat capacity of the glass at the same temperature as the melt datum (e.g. Toplis *et al*., 2001; Webb, 2011). An alternative method to calculate C_p^{conf} is to take $C_{pg}(T_f)$ as the limiting value of the glass (vibrational) heat capacity as it can be assumed that the vibrational contribution to the heat capacity value is constant above T_f; or to assume that the vibrational contribution to C_{pg} = 3nR – the Dulong-Petit limit to the vibrational heat capacity of a glass; for n = atoms per gram formula weight (see Richet and Bottinga, 1995; Toplis et al., 2001). The Dulong-Petit limit for the present glasses with n ~ 2.95 is ~74 J mol^{-1} K^{-1}. As seen in Fig. 1, this is close to the heat capacity value at which the onset of the glass transition peak occurs for the compositions studied here.

The configurational entropy at T_g^{12} was calculated from the viscosity data using the equation of Richet (1984):

$$\log_{10}\eta(T) = A_e + \frac{B_e}{\ln 10 \cdot \left[S_{conf}\left(T_g^{12}\right) + \int_{T_g^{12}}^{T} \frac{C_p^{conf}}{T} dT \right] \cdot T}. \qquad (5)$$

with C_p^{conf} calculated using the extrapolation of the Maier-Kelley equation. The resulting C_p^{conf} and $S_{conf}(T_g^{12})$ values are given in Table 5 and shown in Figure 5. The variation in C_p^{conf} and $S_{conf}(T_g^{12})$ are shown as a function of chlorine content. As the addition of chlorine to the melt also causes the Fe^{2+}/Fe^{tot} to vary it is not clear whether the changes in these thermodynamic parameters are solely due to the addition of chlorine or also a function of the oxidation state of the iron in the melts. The (semi-)parallel curves seen for the Fe-bearing and the Fe-free glasses in Fig. 5 would indicate that chlorine has a larger effect on C_p^{conf} and $S_{conf}(T_g^{12})$ than the oxidation state of iron. The $S_{conf}(T_g^{12})$ data were calculated using A= -3.7 (Toplis, 1998; Russell et al., 2003) as there are not enough viscosity data at high temperatures to constrain this value in the fitting procedure.

3.3 Viscosity

The addition of 1.41 mol% Cl_2O_{-1} to the basalt composition melt results in a 0.5 log unit decrease in viscosity in the high viscosity range investigated here (see Fig. 6). The viscosity data for each series of melts shown in Fig. 6 have been normalised to the temperature at which the viscosity of the Cl-free endmember is 10^{12} Pa s. This decrease in viscosity is in contrast to the 0.9 log unit increase in viscosity observed by Baasner et al. (2013) upon the addition of 0.55 mol% Cl_2O_{-1} to an Fe-free peralkaline Na_2O-CaO-Al_2O_3-SiO_2 melt; and the 0.2 log unit increase in viscosity observed by Zimova & Webb (2006) upon the addition of 0.6 mol% Cl_2O_{-1} to a peralkaline iron-bearing Na_2O-Al_2O_3-SiO_2 melt. This decrease in viscosity due to the addition of chlorine is also in contrast to the 0.2 $\log_{10}$ unit increase in viscosity observed here when 0.8 mol% Cl_2O_{-1} is added to an iron-free haplobasaltic melt. It must be noted that there may also be small variations in viscosity occurring in these melts due to variations in the water content (65-255 ppm) as the model of Robert et al. (2013) calculates that an increase of 100 ppm water to nominally anhydrous calc-alkaline basaltic andesite melt will result in up to 0.1 $\log_{10}$ unit decrease in viscosity in the high viscosity range.

3.4 Fe^{2+}/Fe^{tot}

The major difference between the melt of Baasner et al. (2013), the present haplobasalt, and the present basalt melt is the presence of iron. The importance of the iron content of the basalt melt becomes apparent when comparing the Fe^{2+}/Fe^{tot} for the chlorine-free and chlorine-bearing compositions. As seen in Table 3 and Fig. 4, the Fe^{2+}/Fe^{tot} ratio increases linearly with increasing Cl_2O_{-1} content – for the fluorine-free compositions. The line in Fig. 4 is that calculated assuming that each Cl^- added to the basaltic composition results in the conversion of a Fe^{3+} to a Fe^{2+}. This reaction would explain the decrease in viscosity which

occurs upon the addition of chlorine. It is not necessarily the structural position of the chlorine which results in a decrease in viscosity, rather it is the replacement of a network-forming Fe^{3+} with a network-modifying Fe^{2+}, which occurs in the presence of chlorine.

Liebske et al. (2003) have shown that an increase in $Fe^{2+}/\Sigma Fe_{tot}$ from 0.42 to 0.79 results in a decrease in viscosity of 1.7 log units from 10^{10} to $10^{8.3}$ Pa s for their andesitic composition (8 wt% FeO) melt.

The same dependency of Fe^{2+}/Fe^{tot} on the amount of added halogen does not apply for the fluorine-bearing melt (see Fig. 4). However, taking the above discussion to apply also to the Fe^{2+}/Fe^{tot} in these 2 melts as a function of Cl_2O_{-1} content, one calculates that 1 in 4 of the added Cl atoms results in the conversion of one Fe^{3+} to an Fe^{2+} in the F-bearing melt. The presence of fluorine therefore appears to hinder the reducing action of chlorine in this basaltic composition melt.

The effect of chlorine on the viscosity of a haplobasaltic composition was also investigated. The composition of this iron-free melt was calculated by replacing the Fe^{3+} of the original halogen-free basalt with Al^{3+} and the Fe^{2+} with Mg^{2+}. The amount of chlorine that could be introduced into this melt is half that which could be added to the iron-bearing composition. This implies that the solubility of chlorine is not a function of the concentration of divalent atoms, but a function of the concentration of iron atoms in the melt. It is not clear if Fe^{2+} or Fe^{3+} ions increase the solubility of chlorine, however, the fact that the addition of Cl increases the relative proportion of ferrous iron could be taken as evidence in favour of a preference of Cl for Fe^{2+} rather than Fe^{3+}. Chlorine increases the viscosity of the present iron-free melt. This is in agreement with the rheology measurements of Baasner et al. (2013) on their Na_2O-CaO-Al_2O_3-SiO_2 composition melt.

Comparison of the effect of chlorine on the viscosity of iron-bearing and iron-free melts suggests that the structural position of chlorine in the melt acts to increase the viscosity of the melt. However, the presence of chlorine results in a reduction of the iron in the melt and therefore an increase in the network-modifier/network-former ratio which acts to reduce viscosity.

The other melt composition investigated here and shown in Fig. 6 is a fluorine-bearing basalt to which chlorine is added. The addition of fluorine to the present basalt results in a decrease in viscosity, as observed in all other composition melt. However, the addition of chlorine to the fluorine-bearing basalt results in an increase in viscosity; and a slight increase in

Fe^{2+}/Fe^{tot}. This increase in viscosity occurs despite the presence of iron in the melt. The changes in viscosity due to the addition of chlorine to a fluorine-free and a fluorine-bearing basalt supports the hypothesis that the structural position taken by the Cl^- in the melt acts to increase viscosity; but that the presence of the chlorine reduces a Fe^{3+} to an Fe^{2+} thus increasing the number of network-modifiers, which acts to decrease the viscosity. The presence of fluorine acts to dampen the effect of chlorine.

The remaining set of literature data shown in Fig. 6 is that of Zimova & Webb (2006) in which the addition of 0.22-0.54 mol% Cl_2O_{-1} results in a ~0.2 $\log_{10}$ unit increase in viscosity (except for one composition in which a viscosity decrease is observed. It is not clear why the addition of chlorine to this one peralkaline composition results in a decrease in viscosity.) The addition of chlorine to the melts of Zimova and Webb (2006) resulted in a 0.04 increase in Fe^{2+}/Fe^{tot} from ~0.15. This increase in the proportion of ferrous iron due to the addition of chlorine is about half of that observed for the present basaltic composition melts.

The increase in viscosity observed by Zimova and Webb (2006) due to the addition of chlorine to a melt with a small amount of iron (~4 mol% FeO_{tot}), in comparison to the decrease in viscosity observed in the present melts with 8 mol% FeO_{tot} further supports the hypothesis that there are competing effects on viscosity due to the structural position of the added chlorine (increase in viscosity) and the increase in the total amount of ferrous iron due to the presence of chlorine (decrease in viscosity).

More importantly, it is clearly shown here that the addition of chlorine to the present basaltic melt results in an increase in Fe^{2+}/Fe^{tot} from 0.13 for the chlorine-free glass to 0.43 for the glass with 1.41 mol% Cl_2O_{-1}. Taking the theoretical relationship between oxidation state and fO_2;

$$\log_{10} \frac{Fe^{3+}}{Fe^{2+}} \text{ (atoms)} \propto 0.25 \log_{10}(fO_2) \quad (6)$$

for an ideal solution (Paul and Douglas, 1965; see Mysen and Richet, 2005 for a discussion) the change in Fe^{2+}/Fe^{tot} from 0.13 to 0.43, at a constant log fO_2 in air, due to the addition of chlorine, would normally indicate a 3 $\log_{10}$ unit lower log fO_2 than that of the source region of the melt.

Mysen et al. (1985) found experimentally that the -0.25 parameter ranged from -0.15 to -0 37 for alkaline-earth aluminosilicates; which would translate to the calculation of a 5 to 2 order of

magnitude decrease in fO_2 for the present chlorine-bearing glasses. The increase in Fe^{2+}/Fe^{tot} resulting from the addition of 0.1 mol% Cl_2O_{-1}, would therefore be interpreted to be due to a decrease of 0.5 to 0.2 in $\log_{10} fO_2$.

Conclusion

The presence of chlorine in the present basaltic composition glass acts to reduce the Fe^{3+} in the melt. This has not been observed previously.

The viscosity data presented here show that the addition of chlorine decreases the viscosity of iron-bearing aluminosilicate melts; but increases the viscosity of iron-free aluminosilicate melts. This is in general agreement with literature data. The rheology data for the different compositions melts investigated here and from the literature implies that the structural position of Cl^{-1} in the melt acts to increase viscosity; but the reducing effect of Cl^{-1} on Fe^{3+} acts to decrease viscosity. The NMR study of Baasner et al. (2013) found that chlorine does not directly substitute for an oxygen bonded to tetrahedrally coordinated Si or Al, but uses the network modifying cations to form salt-like coordination structures; thus increasing the viscosity of iron-free peralkaline Na_2O-CaO-Al_2O_3-SiO_2 melts.

It is possible that at small concentrations of chlorine (or iron), these two effects balance each other or indeed the effect of an increase in the amount of network modifiers on viscosity is less than the structural effect of adding chlorine. It is not clear how the presence of fluorine protects the Fe^{3+} ions from the reducing effect of chlorine.

Acknowledgements

I particularly want to thank Burkhard Schmidt for the MIR water content measurements.
The VENTuRE survey was principally funded by the Marine Institute under the 2011 Ship-Time Programme of the National Development Plan and by the National Geographic Society, a special thanks goes to the RV Celtic Explorer officers and crew, ROV technical team and onshore support team in the Marine Institute and P&O Maritime.
The crystal-free basalt glass samples were provided by Boris Dorschel of the Irish scientific expedition VENTuRE aboard the national research vessel *RV Celtic Explorer.* The authors were introduced to each other by John Benzie.

References

Baasner, A., Schmidt, B.C., Webb, S.L., 2013. Compositional dependence of the rheology of halogen (F, Cl) bearing melts, Chemical Geology, 346, 172-183. http://dx.doi.org/10.1016/j.chemgeo.2012.09.020

Behrens, H., Hahn, M., 2009. Trace element diffusion and viscous flow in potassium-rich trachytic and phonolitic melts, Chemical Geology, 259, 63-77.

Black, B.A., Elkins-Tanton, L.T., Rowe, M.C., Ukstins Peate, I., 2012. Magnitude and consequences of volatile release from the Siberian Traps, Earth and Planetary Science Letters, 317–318, 363–373.

Byers C.D., Garcia M.O., Muenow D.W., 1986. Volatiles in basaltic glasses from the East Pacific Rise at 21°N: implications for MORB sources and submarine lava flow morphology, *Earth and Planetary Science Letters,* 79 (1986) 9-20

Briais, A., Sloan, H., Parson, L.M., Murton, B.J., 2000. Accretionary processes in the axial valley of the Mid-Atlantic Ridge 27° N – 30° N from TOBI side-scan sonar images, Marine Geophysical Research, 21, 87-119.

Davi, M., Behrens, H., Vetere, F., De Rosa, R., 2009. The viscosity of latitic melts from Lipari (Aeolian Islands, Italy): Inference on mixing-mingling processes in magmas, Chemical Geology, 259, 89-97.

Di Genova, D., Romano, C., Hess, K.-U., Vona, A., Poe, B.T., Giordano, D., Dingwell, D.B., Behrens, H. 2013. The rheology of peralkaline rhyolites from Pantelleria Island. Journal of Volcanology and Geothermal Research, 249, 201–216.

Dingwell, D.B., Hess, K.U., 1998. Melt viscosities in the system Na-Fe-Si-O-F-Cl: Contrasting effects of F and Cl in alkaline melts ,American Mineralogist, 83, 1016-1021.

Dingwell, D.B., Knoche, R., Webb, S.L. 1993. The effect of F on the density of haplogranitic melt, American Mineralogist, 78, 325-330.

Getson, J.M., Whittington, A., 2007. Liquid and magma viscosity in the anorthite-forsterite-diopside-quartz system and implications for the viscosity-temperature paths of cooling magmas, Journal of Geophysical Research, 112, B10203.

Giordano, D., Dingwell, D.B., 2003. Viscosity of hydrous Etna basalt: implications for Plinian-style basaltic eruptions, Bulletin of Volcanology, 65. 8-14.

Hobiger, M., Sonder, I., Buettner, R., Zimanowski, B., 2011. Viscosity characteristics of selected volcanic rock melts, Journal of Volcanology and Geothermal Research, 200, 27-34.

Ishibashi, H., Sato, H., 2010. Bingham fluid behavior of plagioclase-bearing basaltic magma: Reanalyses of laboratory viscosity measurements for Fuji 1707 basalt, Journal of Mineralogical and Petrological Science, 105, 334-339.

Koleszar, A.M., Saal, A.E., Hauri, E.H., Nagle, A.N., Liang, Y., Kurz, M.D., 2009. The volatile

contents of the Galapagos plume; evidence for H_2O and F open system behavior in melt inclusions, Earth and Planetary Science Letters, 287, 442-452.

Liebske, C., Behrens, H., Holtz, F., Lange, R.A., 2003. The influence of pressure and composition on the viscosity of andesitic melts, Geochimica et Cosmochimica Acta, 67, 473–485.

Liu, Q., Lange, R.A., 2006. The partial molar volume of Fe_2O_3 in alkali silicate melts: Evidence for an average Fe^{3+} coordination number near five, American Mineralogist, 91, 385-393.

Maier, C.G., Kelley, K.K., 1932. An equation for the representation of high-temperature heat content data, Journal of the American Chemical Society, 54, 3243-3246.

Misiti, V., Vetere, F., Freda, C., Scarlato, P., Behrens, H., Mangiacapra A., Dingwell, D.B., 2011. A general viscosity model of Campi Flegrei (Italy) melts, Chemical Geology, 290, 50-59.

Misiti, V.F., Vetere, A., Mangiacapra, A., Behrens, H., Cavallo, A., Scarlato, P., Dingwell, D.B., 2009. Viscosity of high-K basalt from the 5th April 2003 Stromboli paroxysmal explosion, Chemical Geology, 260, 278-285.

Moynihan, C.T., Easteal, A.J., DeBolt, M.A., Tucker, J. 1976. Dependence of the fictive temperature of glass on cooling rate, Journal of the American Ceramic Society, **59**, 12 -16.

Mysen, B.O. and Richet, P. 2005. Silicate Glasses and Melts: Properties and Structure, pp 548, Elsevier, Amsterdam.

Mysen, B.O., Virgo, D., Neumann, E.R., Seifert, F. 1985. Redox equilibria and the structural states of ferric and ferrous iron in melts in the system CaO-MgO-Al_2O_3-SiO_2-FeO: relationships between redox equilibria, melt structure and liquidus phase equilibria, American Mineralogist, Volume 70, 317-331.

Paterson, M.S., 1982. The determination of hydroxyl by infrared absorption in quartz, silicate glasses and similar materials. Bull. Mineral. 105, 20-29.

Paul, A., Douglas, R.W., 1965. Ferrous-ferric equilibrium in binary alkali silicate glasses, Physics and Chemistry of Glasses, 6, 207-211.

Pocklington, H.C., 1940. Rough measurement of high viscosities, Proceedings of the Cambridge Philosophical Society, 36, 507-508.

Richet, P., 1984. Viscosity and configurational entropy of silicate melts, Geochimica Cosmochimica Acta, 48, 471–483.

Richet, P. and Bottinga, Y. 1995. Rheology and configurational entropy of silicate melts, in Structure, Dynamics and Properties of Silicate Melts, Reviews in Mineralogy, 32, 67-93.

Robert, G., Whittington, A.G., Stechern, A., Behrens, H., 2013. The effect of water on the viscosity of a synthetic calc-alkaline basaltic andesite, Chemical Geology, 346, 135–148.

le Roex, A.P., Frey, F.A., Richardson, S.H., 1996. Petrogenesis of lavas from the AMAR

Valley and Narrowgate region of the FAMOUS Valley, 36°–37°N on the Mid-Atlantic Ridge, Contributions to Mineralogy and Petrology, 124, 167-184.

Robie, R.A., Hemingway, B.S., Fischer, J.R., 1978. Thermodynamic properties of minerals and related substances at 298.15 K and 1 bar (10^5 pascals) pressure and at higher temperatures. US Geological Survey Bulletin.

Russell, J.K., Giordano, D., Dingwell, D.B., 2003. High-temperature limits on viscosity of non-Arrhenian silicate melts, American Mineralogist, **88**, 1390–1394.

Searle, R.C., Murton, B.J., Achenbach, K., LeBas, T., Tivey, M., Yeo, I., Cormier, M.H., Carlut, J., Ferreira, P., Mallows, C., Morris, K., Schroth, N., van Calsteren, P., Waters, C., 2010. Structure and development of an axial volcanic ridge: Mid-Atlantic Ridge, 45° N, Earth and Planetary Science Letters, 299, 228-241.

Stretch, R.C., Mitchell, N.C., Portaro, R.A., 2006. A morphometric analysis of the submarine volcanic ridge south-east of Pico Island, Azores, Journal of Volcanology and Geothermal Research, 156, 35-54.

Toplis, M.J., 1998. Energy barriers to flow and the prediction of glass transition temperatures of molten silicates, American Mineralogist, **83**, 480–490.

Toplis, M.J., Gottsmann, J., Knoche, R., Dingwell, D.B. 2001. Heat capacities of haplogranitic glasses and liquids, Geochimica Cosmochimica Acta, **65**, 1685–1694.

Vetere, F., Behrens, H., Holtz, F., Neuville, D.R., 2006. Viscosity of andesitic melts - new experimental data and a revised calculation model, Chemical Geology, **228**, 233-245.

Vetere, F., Behrens, H., Misiti, V., Ventura, G., Holtz, F., De Rosa, R., Deubener, J., 2007. The viscosity of shoshonitic melts (Vulcanello Peninsula, Aeolian Islands, Italy): Insight on the magma ascent in dikes, Chemical Geology, **245**, 89-102.

Vetere. F., Behrens, H., Schuessler, J.A., Holtz, F., Misiti, V., Borchers, L., 2008. Viscosity of andesite melts and its implication for magma mixing prior to Unzen 1991-1995 eruption, Journal of Volcanology and Geothermal Research, 175, 208-217.

Villeneuve. N., Neuville, D.R., Boivin, P., Bacheery, P., Richet, P., 2008. Magma crystallization and viscosity: A study of molten basalts from the Piton de la Fournaise volcano (La Reunion island), Chemical Geology, 256, 242-251.

Wanless, V.D., Perfit, M.R., Ridley, W.I., Wallace, P.J., Grimes, C.B., Klein, E.M., 2011. Volatile abundances and oxygen isotopes in basaltic to dacitic lavas on mid-ocean ridges: The role of assimilation at spreading centers, Chemical Geology, 287, 54-65.

Webb, S.L., 2011. Configurational heat capacity and viscosity of (Mg, Ca, Sr, Ba)O-Al_2O_3-SiO_2 melts, European Journal of Mineralogy, 23, 487-497.

Wheeler, A.J., Benzie, J.A., Carlsson, J., Collins, P.C., Copley, J., Gree, D., Murton, B., Dorschel, B., Antoniacomi, A., Coughlan, M., Judge, M., Lim, A., Morris, K., Nye, V., 2011a.

Moytirra: a newly discovered hydrothermal vent field on the mid-Atlantic Ridge between the Azores and Iceland. InterRidge News, 20, 37 - 39.

Wheeler, A.J. & Science Party, 2011b. Cruise Report CE11009: RV Celtic Explorer & Holland I ROV. VENTuRE Survey: VENTs and REefs deep-sea ecosystem study of the 45° North MAR hydrothermal vent field and the cold-water coral Moira Mounds, Porcupine Seabight - 11th July – 4th August, 2011. Unpublished Report, University College Cork, Ireland.

Wheeler, A.J., Murton, B., Copley, J., Lim, A., Carlsson, J., Collins, P., Dorschel, B, Green, D., Judge, M., Nye, V., Benzie, J., Antoniacomi, A., Coughlan, M., Morris, K., 2013. Moytirra: first known deep-sea hydrothermal vent field in the slow spreading MAR north of Azores. Geochemistry, Geophysics, Geosystems, submitted.

Whittington, A., Richet, P., Holtz, F., 2000. Water and the viscosity of depolymerized aluminosilicate melts, Geochimica Cosmochimica *Acta*, 64, 3725-3736.

Whittington, A.G., Hellwig, B.M., Behrens, H., Joachim, B., Stechern, A., Vetere, F., 2009. The viscosity of hydrous dacitic liquids: implications for the rheology of evolving silicic magmas, *Bull. Volc*., 71 185-199.

Zimova, M., Webb, S.L., 2006. The effect of chlorine on the viscosity of Na_2O-Fe_2O_3-Al_2O_3-SiO_2 melts, American Mineralogist, 91, 344-352.

Table 1. Composition (in mol%) of the volcanic glass from Station V24 (45° 28.7'N/27° 51.0'W) from the Venture project. The composition was determined by electron microprobe.

mol%	V24
SiO_2	56.90
TiO_2	1.09
Al_2O_3	9.89
MgO	13.26
CaO	12.43
Fe_2O_3	4.40
Na_2O	1.69
K_2O	0.17
MnO	0.16

Table 2. Composition of the present glasses (in atom%) determined by electron microprobe. Standards were: albite – Na; sanidine – K; wollastonite – Si, Ca; TiO_2 – Ti; rhodonite – Mn; hematite – Fe; olivine- Ng; anorthite – Al; NaCl – Cl; topaz – F. The compositions were obtained for 15 kV voltage, 10 μm beam diameter, 12 nA current on a JEOL JXA 8900 RL. Data are the average of 10 analyses of each glass. Data were ZAF corrected.

atom%	X24	X24 Cl-1	X24 Cl-2	X24 F	X24 Cl-1 F	HX24	HX24 Cl-1	HX24 Cl-2
Si	47.00	47.51	47.51	45.45	45.68	46.99	47.10	47.10
Na	4.72	3.96	3.39	4.46	3,12	4.67	4.43	2.52
K	0.36	0.30	0.24	0.35	0.20	0.42	0.35	0.30
Ti	0.94	0.94	0.94	0.87	0.92	0.94	0.93	0.93
Al	16.76	16.83	16.86	16.05	16.22	23.32	23.35	23.29
Mg	11.85	11.78	11.75	11.33	11.44	12.76	12.75	12.67
Ca	10.69	10.63	10.58	10.20	10.33	10.70	10.57	10.72
Fe	7.50	6.90	6.15	7.18	6.09	0.03	0.03	0.03
Mn	0.14	0.13	0.12	0.14	0.12	0.15	0.13	0.11
Cl	-	0.99	2.44	-	0.96	-	0.36	1.33
F	-	-	-	3.96	4.92	-	-	-

Table 3. Composition of the present glasses (in mol%) determined by electron microprobe; together with Fe^{2+}/Fe^{tot}, NBO/T, density of the glasses, and their molar mass and molar volume. The compositions were obtained for 15 kV voltage, 10 μm beam diameter, 12 nA current on a JEOL JXA 8900 RL. Data are the average of 10 analyses of each glass.

mol%	X24	X24 Cl-1	X24 Cl-2	X24 F	X24 Cl-1 F	HX24	HX24 Cl-1	HX24 Cl-2
SiO_2	54.79	55.01	54.75	53.73	53.84	54.80	54.94	55.25
Na_2O	2.75	2.29	1.95	2.64	1.84	2.72	2.58	1.48
K_2O	0.21	0.17	0.14	0.21	0.12	0.24	0.20	0.18
TiO_2	1.10	1.09	1.08	1.03	1.08	1.10	1.08	1.09
Al_2O_3	9.77	9.74	9.71	9.49	9.56	13.60	13.62	13.66
MgO	13.81	13.64	13.54	13.39	13.48	14.88	14.87	14.86
CaO	12.46	12.31	12.19	12.06	12.18	12.48	12.33	12.57
FeO	1.10	2.00	3.06	1.41	1.41	-	-	-
Fe_2O_3	3.82	3.00	2.01	3.54	2.88	-	-	-
MnO	0.16	0.15	0.14	0.17	0.14	0.17	0.15	0.13
Cl_2O_{-1}	-	0.57	1.41	-	0.57	-	0.21	0.78
F_2O_{-1}	-	-	-	2.34	2.90	-	-	-
Fe_2O_3 wt% chem/ems	1.00	1.04	1.04	1.03	1.08			
Fe^{2+}/Fe^{tot}	0.126±0.020	0.250±0.015	0.432±0.039	0.166±0.018	0.197±0.018	-	-	-
H_2O (ppm)	65	255	186	229	75	72	110	120
NBO/T[a]	0.407	0.437	0.487	0.417	0.463	0.407	0.397	0.372
NBO/T[b]	0.407	0.422	0.451	0.359	0.373	0.407	0.392	0.353
γ	0.692	0.702	0.726	0.696	0.711	0.692	0.689	0.681
ρ g cm^{-3}	2.758	2.749	2.736	2.775	2.753	2.641	2.639	2.637
molar mass g	65.227	64.486	63.577	64.085	63.139	62.705	62.677	62.641
molar volume cm^3 mol^{-1}	23.65	23.46	23.24	23.09	22.93	23.74	23.75	23.75

Fe_2O_3 wt% chem./ems - wet chemistry value / electron microscopy value of the iron content calculated as all Fe_2O_3.
a – NBO/T calculated ignoring the presence of chlorine and fluorine.
b - NBO/T calculated assuming each chlorine and fluorine replace an oxygen.
γ – $[Na_2O+K_2O+MnO+FeO+CaO+MgO]/[Na_2O+K_2O+MnO+FeO+CaO+MgO+Al_2O_3+Fe_2O_3]$ in mol. fractions
ρ – measurements have and error of ±0.003 g cm^{-3}

Table 4. Viscosity data for the eight melts. The error in temperature is 0.5C. The error in viscosity is 0.06 $\log_{10}$ Pa s.

X24		X24 Cl-1		X24 Cl-2		X24 F	
T °C	Viscosity $\log_{10}$ Pa s	T °C	Viscosity $\log_{10}$ Pa s	T °C	Viscosity $\log_{10}$ Pa s	T °C	Viscosity $\log_{10}$ Pa s
668.0	12.47	653.2	12.61	643.4	12.97	633.3	12.37
669.6	12.40	663.9	12.18	659.9	12.23	643.7	11.84
677.2	12.04	676.1	11.68	673.0	11.67	652.7	11.53
684.7	11.69	683.2	11.31	692.4	10.82	662.4	10.90
691.0	11.25	694.9	10.93	702.8	10.52	676.3	10.37
695.6	11.29	697.6	10.61	703.9	10.46	677.8	10.61
705.5	10.64	703.7	10.45	722.7	9.73	681.4	10.15
712.1	10.52	714.7	10.22	733.8	9.58	692.3	9.78
714.7	10.61	718.5	9.97	753.9	8.79	706.5	9.40
725.0	9.97	726.8	9.62	770.8	8.29	719.8	9.04
725.2	10.12	739.5	9.16			732.4	8.60
727.9	9.77	752.9	8.83				
735.3	9.60	759.5	8.64				
736.7	9.52						
737.2	9.61						
751.2	9.04						
753.1	8.95						
764.5	8.72						
X24 F Cl-1		HX24		HX24 Cl-1		HX24 Cl-2	
T °C	Viscosity $\log_{10}$ Pa s	T °C	Viscosity $\log_{10}$ Pa s	T °C	Viscosity $\log_{10}$ Pa s	T °C	Viscosity $\log_{10}$ Pa s
645.6	12.16	710.5	12.77	713.3	12.69	719.1	12.60
658.1	11.50	724.2	12.13	722.5	12.16	734.0	11.96
660.3	11.46	732.9	11.82	733.6	11.74	744.7	11.51
674.4	10.76	741.3	11.46	746.5	11.22	755.8	11.09
683.2	10.59	752.6	10.98	754.8	10.99	761.9	10.85
695.1	10.25	762.9	10.69	770.2	10.40	774.4	10.44
700.0	9.8	769.0	10.42	781.5	10.02	782.9	10.10
711.1	9.45	780.4	9.94	795.8	9.55	792.6	9.65
721.4	9.16	790.4	9.62	806.2	9.07	801.8	9.35
728.1	8.67	805.2	9.14	821.2	8.70	817.0	8.98
		818.9	8.74				

Table 5.

Parameters for the Arrhenian fit to the viscosity data, together with T_g^{12} – the temperature at which the melt has a viscosity of 10^{12} Pa s, m – fragility of the melt, $C_{pl}(T)$ – the relaxed, liquid heat capacity at the highest measured temperature; C_p^{conf} – the measured configurational heat capacity of the melt, $S_{conf}(T_g^{12})$ - the calculated configuration entropy of the melt at T_g^{12}, the parameter B_e, and T_f^{20} – the calculated fictive temperature for a sample which had been cooled at a rate of 20 K min^{-1} (and reheated at a rate of 20 K min^{-1}).

	A $\log_{10}$ Pa s	B $\log_{10}$ Pa s K	T_g^{12} K	η @T_g^{12} [a] $\log_{10}$ Pa s	m	$C_{pl}(T)$ J mol^{-1} K^{-1}	$C_p^{conf}(T_g)$ J mol^{-1} K^{-1}	$S_{conf}(T_g^{12})$ J mol^{-1} K^{-1}	B_e kJ mol^{-1}	T_f^{20} K
X24	-28.97 ± 0.85	38,932 ± 838	950	12.00	41	99.79 ±0.33	20.66 ±0.44	10.93 ±0.35	376 ±11	940
X24 Cl-1	-26.57 ± 0.74	36,247 ± 722	940	11.58	39	97.20 ±0.28	19.74 ±0.11	11.50 ±0.34	391 ±11	931
X24 4Cl-2	-25.18 ± 0.73	34,862 ± 688	938	11.52	37	94.14 ±0.20	18.35 ±0.31	11.45 ±0.30	388 ±11	930
X24 F	-25.70 ± 1.32	34,381 ± ,1257	912	12.00	40	99.10 ±0.93	21.40 ±0.91	12.64 ±0.66	418 ±21	908
X24 F Cl-1	-27.86 ± 1.26	36,705 1,213	921	12.39	40	97.44 ±0.10	20.52 ±0.54	11.24 ±0.70	375 ±22	907
HX24	-28.01 ± 0.43	40,047 ± 471	1,001	12.00	40	96.46 ±0.22	18.86 ±0.60	10.55 ±0.20	382 ± 7	998
HX24 Cl-1	-27.31 ± 0.60	39,341 ± 617	1,001	12.00	39	96.37 ±0.33	18.65 ±0.40	10.70 ±0.30	387 ±10	1000
HX24 Cl-2	-28.45 ± 0.62	40,688 ± 645	1,006	12.20	40	94.05 ±0.33	18.17 ±0.09	9.83 ±0.26	358 ± 9	1007

T_g^{12} and T_f^{20} have a standard deviation of ±2 K

m = B/T_g (Toplis et al., 1997), and has a standard deviation of ±1

a – η @T_g^{12} - the viscosity measured in the halogen-bearing melt at the same temperature as the halogen-free melt has a viscosity of 10^{12} Pa s

Table 6. The parameters of the fits to the partial molar volume calculation for the rest glass with added chlorine and fluorine, and variable Fe^{2+}/Fe^{tot} .

	partial molar volume $cm^3\ mol^{-1}$
rest glass	23.08 ± 0.12
Cl_2O_{-1}	36.60 ± 1.55
F_2O_{-1}	3.22 ± 0.27
FeO	9.59 ± 1.26
Fe_2O_3	41.86 ± 2.50

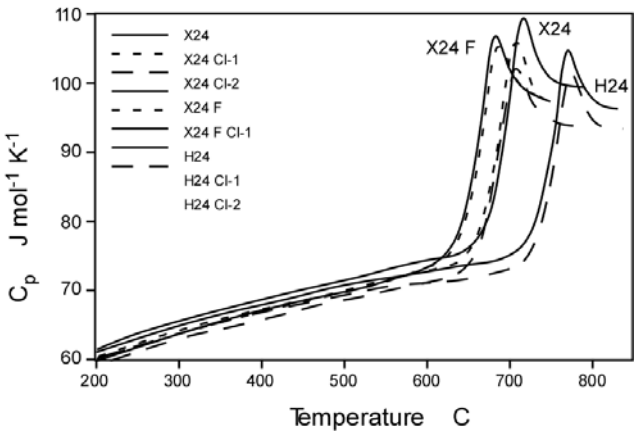


Figure 1. The heat capacity curves for the basalt glasses and melts with added chlorine; together with the heat capacity curves for the basalt with added fluorine, and the haplo-basalt. The curves for the haplo-basalt with chlorine lie on the curve without chlorine. Similarly, the basalt with F and that with both F and Cl show the same curve.

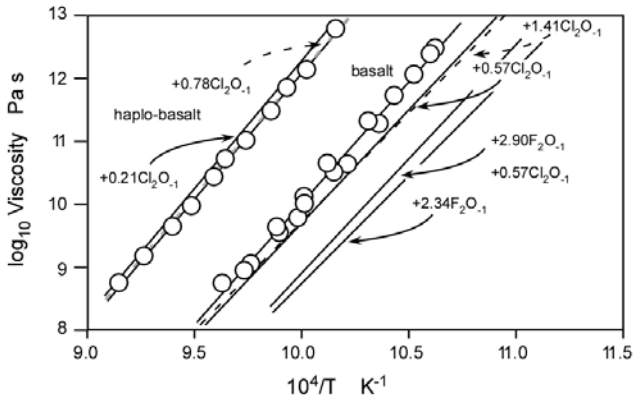


Figure 2. The viscosity data for the eight melts. As the viscosity data lie very close to each other, the data points for the two halogen-free melts are shown; and only the Arrhenian fits to the halogen-bearing melts are shown. The parameters to the Arrhenian fits are given in Table 5.

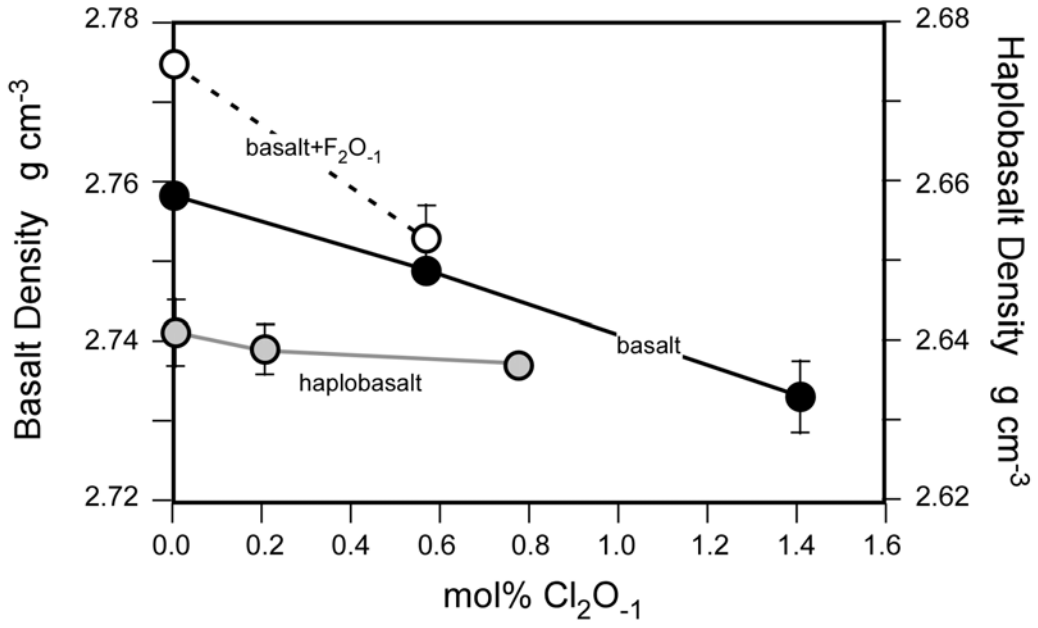


Figure 3. Density of the basalt glass with added chlorine and fluorine; together with the density of the haplobasalt glass.

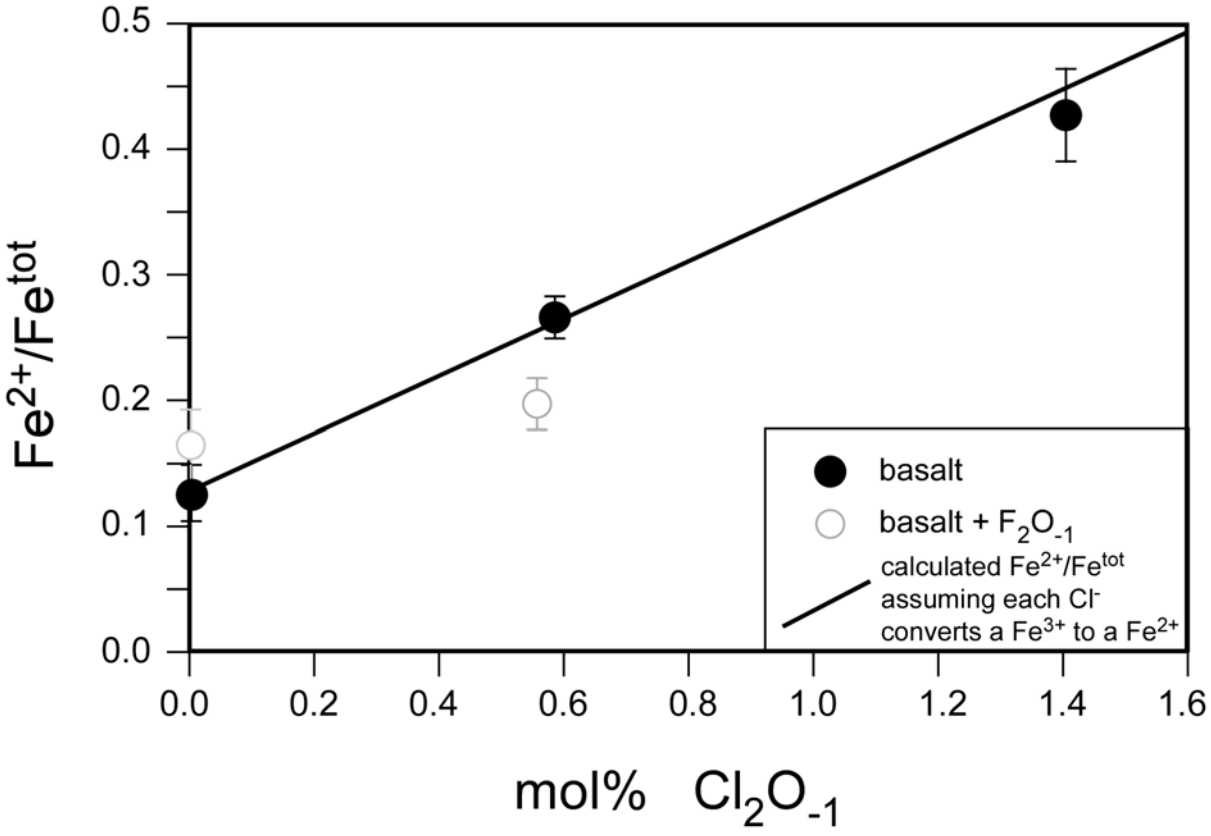


Figure 4. The Fe^{2+}/Fe^{tot} of the glasses as a function of the chlorine content. The straight line is that calaculated on the assumption that each added Cl^{-1} converts a Fe^{3+} to a Fe^{2+}.

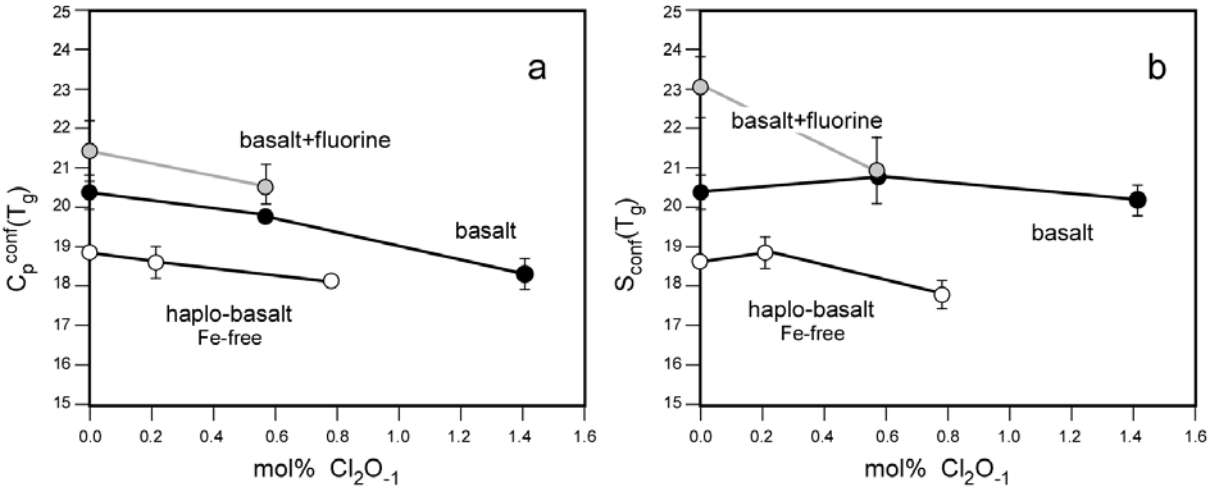


Figure 5. a. The configurational heat capacity (C_p^{conf}) as a function of the chlorine content. b. The configurational entropy of the melts $S^{conf}(T_g^{12})$ at T_g^{12} as a function of the chlorine content.

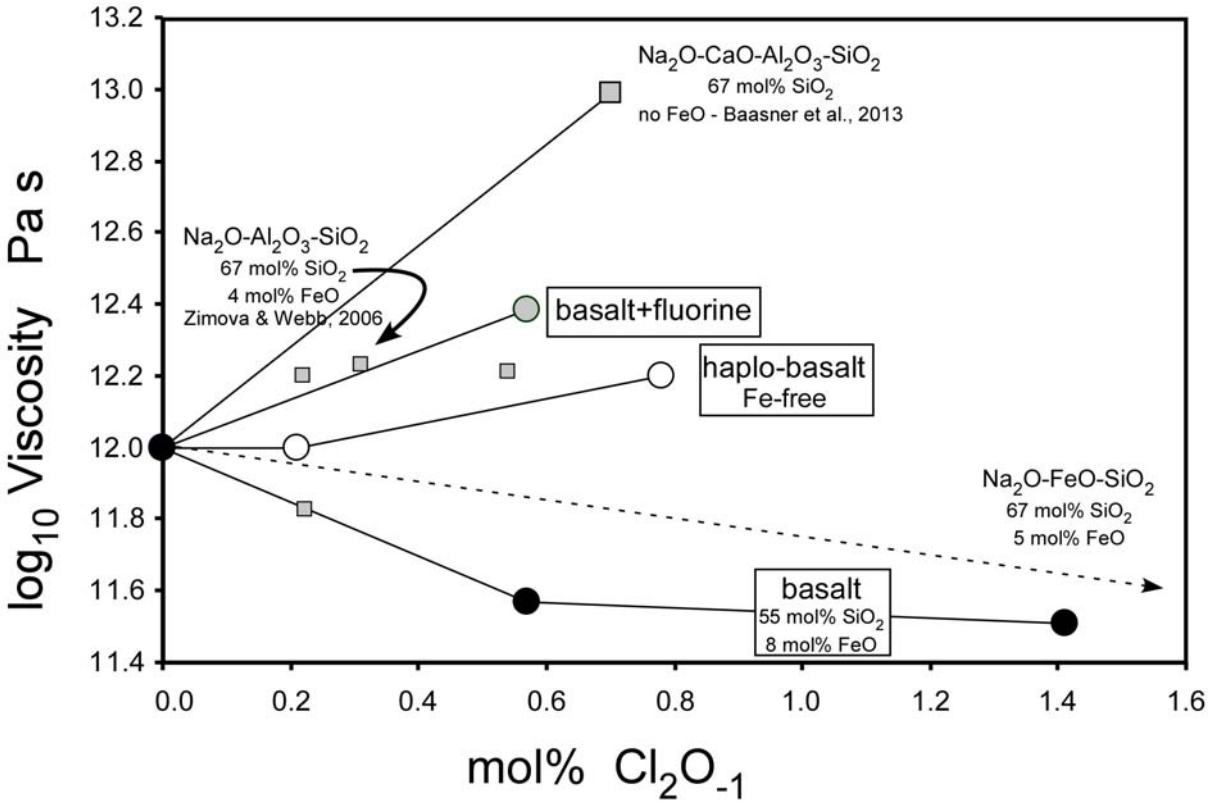


Figure 6. The change in viscosity due to the addition of chlorine and fluorine at the same temperature as the original glass has a viscosity of 10^{12} Pa s. circles – present data; squares – literature data (Zimova and Webb, 2006 – small grey squares, DIngwell and Hess, 1998; Baasner et al., 2013 – large grey square).